Evaluating 3D Earthquake Effects on Sloshing Wave Height of Liquid Storage Tanks Using Finite Element Method

M.A. Goudarzi[1] and S.R. Sabbagh-Yazdi[2]

1. Ph.D. Student, Civil Engineering Dept., K.N. Toosi University of Technology, Tehran, I.R. Iran, email: goudarzi.ma@gmail.com
2. Associate Professor, Civil Engineering Dept., K.N. Toosi University of Technology, Tehran, I.R. Iran

ABSTRACT

The objective of this article is to study the effect of various components of earthquake on sloshing response of liquid storage tanks. First, commonly used theory for unidirectional analysis of liquid behavior in cylindrical tanks was reviewed. Second, the Finite Element Modeling (FEM) strategy which was used to simulate dynamic response of the liquid tank system was described. The FEM was validated using a set of experimental measurements reported by previous researchers. Third, a parametric study for some vertical, cylindrical tanks with different aspect ratios excited by various time series of earthquake accelerations was performed. Each tank was subjected to unidirectional and bidirectional excitations of earthquake accelerations. Fourth, provision suggested by some seismic codes for the estimation of Maximum Sloshing Wave Height (MSWH) were reviewed and the accuracy of the codes prediction was numerically investigated. Finally, the available simplified formulation for evaluating MSWH under unidirectional excitation was extended for bidirectional excitation.

Keywords:
Liquid storage tank;
Seismic analysis;
Bidirectional excitation;
Finite element modeling;
Maximum sloshing wave height

1. Introduction

Liquid sloshing is associated with various engineering problems, such as the liquid flow on the decks of ships, the behavior of liquid in containers, the fuel motion in aircraft and the liquid oscillations in large storage tanks caused by earthquakes. The dynamic characteristic of these systems is greatly affected by the dynamics of the liquid free-surface motion and it is very important regarding to the safety of transportation systems, human's life and environmental issues.

Large amplitude sloshing flows considered in engineering applications are usually followed by impact of liquid at the side wall and top surface of fluid containers. Many studies for the sloshing and impact of liquid on marine industries were carried out in the 1970*s* and early 1980s for the design of *LNG* carriers and some numerical computations have been reported [1-3]. Most of the studies at this time were reported for the two dimensional (2*D*) flows. However, some Japanese researchers continued the studies on the sloshing phenomenon and several interesting results have been reported for the 3*D* flows [4]. The demand for sloshing analyses is rising again for the design of larger *LNG* carriers which have a greater potential for severe sloshing impact occurrence.

Some other representative works in the field of marine industries which is mostly focused on the application of numerical methods for modeling the sloshing phenomena have been introduced by Wu et al [5] and Faltinsen [6]. Kim [7] and Kim et al [8] also developed numerical method based on the finite difference method. This method has been extended to more complicated geometries, e.g. three-dimensional prismatic tanks. Smoothed-Particle Hydrodynamics *SPH* method has also been applied to various liquid free-surface cases, especially for strongly nonlinear

wave problems. Some extensions or applications of this method can be found in the works of Colagrossi and Landrini [9], Iglesias et al [10], and Oger et al [11]. An unstructured grid based formulation on Arbitrary Lagrangian-Eulerian description was used to model the sloshing behavior in a rectangular tank by Kashiyama et al [12]. Cho and Lee [13] employed the finite element analysis of large amplitude liquid sloshing in two-dimensional tank using the fully non-linear potential flow theory and compared their result with the results of linear theory. A Runge-Kutta discontinuous Galerkin (*RKDG*) finite element method was also performed by Martin [14] to the liquid sloshing problem using the depth-averaged shallow water equations in a rotating frame of reference. In this work, the effect of varying roll angle and other geometry parameters on the resulting maximum moment was investigated.

In the field of civil engineering, the sloshing phenomenon becomes important to seismic design of liquid storage tanks. Due to the requirement to remain functional after a major earthquake event, the seismic performance of liquid storage tanks has been a critical issue in municipal water supply and fire fighting systems. Water supply that is able to immediately follow critical earthquakes is vital. If a water tank collapses during destructive earthquakes the loss of public water supply can have serious consequences. Similarly, failure of tanks storing combustible materials can lead to extensive uncontrolled fires. The fluid sloshing impact causes a serious problem in liquid storage tanks subjected to earthquakes. For example the failure of the floating roof and the fire of oil-storage tanks have been frequently observed [15].

Investigations on the seismic response of liquid storage tanks have been conducted over the past 30 years. Most of the previous investigations focus on proposing mechanical models for computing the seismic response of liquid storage tanks. Historically, mechanical models were first developed for tanks with rigid walls. Housner [16-18] was perhaps the first to propose such a simplified mechanical model for circular and rectangular rigid tanks. His simplified model is a two degree-of-freedom (*DOF*) system for rigid tanks, one *DOF* accounting for the motion of the tank-liquid system, with a part of the liquid being rigidly attached (impulsive mode) and the other *DOF* for the motion of the sloshing liquid (convective mode). The mechanical model of Housner is still widely used with certain modifications for the analysis of rectangular and cylindrical tanks. Wozniak and Mitchell [19] generalized Housner's model for short and slender tanks. Veletsos and Yang [20] used a different approach to propose a similar type of a mechanical model for circular rigid tanks. Subsequently, Haroun and Housner [21] and Veletsos [22] developed mechanical models for flexible tanks. Malhotra et al [23] proposed further simplifications of the mechanical model of Veletsos for flexible tanks.

There is a wide variety of guideline codes for earthquake resistant design of steel liquid storage tanks that use one of the above mechanical models. Notwithstanding a consensus in the codes on the treatment of several aspects of the phenomenon, various other aspects remain controversial or unresolved. One of these aspects is prediction of **Maximum Sloshing Wave Height** (*MSWH*) which is one of the major considerations in the design of liquid storage tanks. *MSWH* is used to provide sufficient freeboard between the liquid surface and the tank roof to prevent sloshing waves from impacting the roof. If the sufficient free board is not provided, the liquid impact to the roof should be considered [24-25].

The focus of this study is primarily on the provisions related to prediction of *MSWH*. The investigation is restricted to the case of fixed roof cylindrical vertical storage tanks. The influence of simultaneous seismic ground motion in two transverse directions to the principal directions of motion is numerically investigated and the predictions of various design guideline codes are assessed by comparing their results with finite element analyses results.

This paper is divided into seven sections. In section 2, the linear water wave theory for a vertical cylindrical tank is summarized. In sections 3 and 4, present *FEM* strategy is introduced and the results of the numerical model are verified by comparing with the experimental measurements and theoretical solutions. Section 5 presents the result of *FEM* for some tanks with various aspect ratios subjected to unidirectional and bidirectional acceleration of reported earthquakes. In section 6, the perditions of several design guideline codes for *MSWH* of typical tanks are evaluated. Extension of practical formulation for bidirectional excitation is presented in section 7. In the final section, conclusions are made from the obtained results of the former sections.

2. Linear Wave Theory for Unidirectional Excitation

The equations of liquid motion for many applications of cylindrical liquid containers have been previously solved with various boundary conditions [26-27]. In this section, the closed-form solution for the hydrodynamic loads and water surface elevation in a cylindrical tank subjected to an earthquake motion has been summarized. The behavior of a cylindrical tank of radius R_0 and height H filled with a fluid of density ρ, having a depth h and subjected to a horizontal acceleration (described by a function of time of ground acceleration $\ddot{v}_g(t)$) have been considered. A cylindrical coordinate system (r,θ,z) has been defined with an origin at the center of the tank bottom and the z axis vertically upward, see Figure (1). The natural periods of shell vibration modes are much shorter than the natural periods of sloshing modes. Therefore the assumption of a rigid tank wall may provide a reasonable accuracy. The liquid is assumed to be inviscid, incompressible, and irrigational. Then the liquid motion may be completely defined by a velocity potential function F for which the boundary-value problem can be defined in cylindrical coordinate as:

$$\frac{\partial^2 F}{\partial r^2}+\frac{1}{r}\frac{\partial F}{\partial r}+\frac{1}{r^2}\frac{\partial F}{\partial \theta^2}+\frac{\partial^2 F}{\partial^2 z}=0 \tag{1}$$

At the free surface of the liquid, the pressure P is constant at all points which yield the free surface boundary condition as:

$$\frac{\partial^2 F}{\partial t^2}+g\frac{\partial F}{\partial z}=0 \tag{2}$$

At the bottom of the tank, the liquid particles have zero vertical velocity which result in the bottom boundary condition as:

$$\frac{\partial F}{\partial z}=0 \tag{3}$$

At the tank lateral surface the liquid particles and the tank wall must have the same velocity:

$$\frac{?F}{?r}=\ddot{v}_g(t)\cos\theta \tag{4}$$

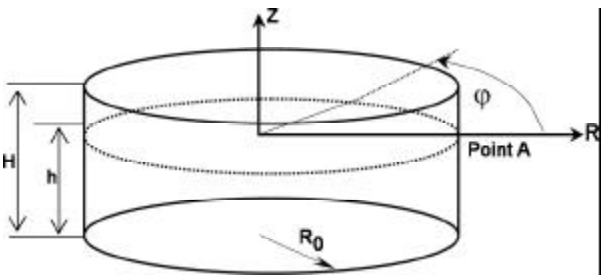

Figure 1. Coordinates and geometrical parameters of cylindrical tank filled by liquid.

The solution for the potential that satisfies the Laplace Eq. (1) the wall condition (4) and the bottom condition (3) is given by Chalhoub [28]:

$$F(r,\theta,z,t)=\sum_{i=1}^{i=?}\chi_i\left[\int_0^t \cos\lambda_i(t-\tau)\,\ddot{v}_g(\tau)\,d\tau\right]\times J_1(n_i r)\,\frac{\cosh n_i(z+h)}{\cosh n_i h}\cos\theta \tag{5}$$

Where J_1 denotes the Bessel function of the first kind of order one and

$$\chi_i=J_1(n_i r)\,\frac{2R_0}{J_1(n_i r)(1-(n_i r)^2)} \tag{6}$$

The parameter λ_i, denotes the i^{th} order of natural circular frequency of free surface mode given by:

$$\lambda_i=\sqrt{(g n_i \tanh n_i h)} \tag{7}$$

The parameters g and h are the gravitational constant and the liquid height in the tank, respectively, and n_i denotes the i^{th} positive root of $J'(nR_0)=0$.

The dynamic pressure and the liquid surface deformation can now be expressed from the velocity potential. The dynamic pressure in the liquid was given by Chalhoub [28]:

$$P_d(r,\theta,z,t)=\rho\frac{?F}{?t}=\rho\cos\theta\,\ddot{v}_g(t)+\rho\cos\theta\sum_{i=1}^{i=?}\chi_i\left[\ddot{v}_g(t)\lambda_i\int_0^t \sin\lambda_i(t-\tau)\,\ddot{v}_g(\tau)d\tau\right]\times J_1(n_i r)\,\frac{\cosh n_i(z+h)}{\cosh n_i h}\cos\theta \tag{8}$$

The free surface displacement can be expressed by:

$$\eta(r,\theta,z,t)=\left(\frac{1}{g}\frac{\partial F}{\partial t}\right)_{(Z=0)}=\frac{\cos\theta}{g}\sum_{i=1}^{i=\infty}\left[\ddot{v}_g(t)-\lambda_i\int_0^t \sin\lambda_i(t-\tau)\,\ddot{v}_g(\tau)\,d\tau\right]\times J_1(n_i r)+\frac{\cos\theta}{g}r\,\ddot{v}_g(t) \tag{9}$$

The pressure at the tank wall in the plane of excitation is obtained for $r=R_0$ and $\theta=0$.

$$P_d(R_0, 0, z, t) = \left(\frac{1}{\rho R_0}\right)\ddot{v}_g(t)\left(1+\sum_{i=1}^{i=\infty} C_i\right) - \left(\frac{1}{\rho R_0}\right)\sum_{i=1}^{i=\infty} C_i \lambda_i I_i(t) \quad (10)$$

The sloshing wave height (*SWH*) and along the diameter of excitation is given by:

$$\eta(R_0, 0, h, t) = \left(\frac{R_0}{g}\right)\ddot{v}_g(t)\left(1+\sum_{i=1}^{i=\infty} C_i'\right) - \left(\frac{R_0}{g}\right)\sum_{i=1}^{i=\infty} C_i' \lambda_i I_i(t) \quad (11)$$

where, the constant C_i' is C_i at the free surface level.

$$C_i = \frac{2}{1-(n_i R_0)^2}\,\frac{cosh n_i (z+h)}{cosh n_i h} \quad (12)$$

The convolution integrals $I_i(t)$ represent the undamped response of freedom oscillator of frequency λ_i subjected to ground acceleration $\ddot{V}_g(t)$.

$$I_i(t) = \int_0^t sin\lambda_i(t-\tau)\,\ddot{v}_g(\tau)\,d\tau \quad (13)$$

Therefore, considering only the first sloshing mode in Eq. (11), the *SWH* could be evaluated based on $A_c(t)$, the absolute acceleration, of the convective *DOF* of mechanical equivalent system as:

$$h(t) = 0.84R\frac{A_c(t)}{g} \quad (14)$$

The above equation is the base of many codes and standards (which was described in section 6) for calculating *MSWH*. In this equation *h* is the wave height, *R* is the radius of the tank and *g* is the gravitational acceleration.

3. Multi-Directional FEM Strategy

All tanks considered in this study are cylindrical steel storage tanks filled by liquid. The Finite Element Model (*FEM*) has been utilized to model the tanks as well as the contained liquid. *ANSYS*, a finite element code, is used to model the tank-fluid system in the three dimensional space under seismic load. Newmark's Method is employed to simulate the time history response analysis during earthquake ground motion. A Rayleigh damping matrix is defined in the two significant modes; the first sloshing (convective) mode and the first horizontal coupled (impulsive) mode. For the sloshing mode, the damping ratio is considered to be 0.5% and for the impulsive mode is defined to be 2.0%. This corresponds to the linear elastic range of steel cylindrical tank. Taking advantage of the symmetry of a cylindrical tank, only the half of each storage tank is modeled for *FEM* analysis under unidirectional earthquake excitation in the direction parallel to the plane of symmetry, see Figure (2b). In contrast, full geometry of the storage tanks was considered for *FEM* analysis of the bidirectional excitation, see Figure (2a). 24 *DOF* quadrilateral elastic shell elements that have both membrane and bending capabilities is provided to model the tank wall. The material property of tank wall is considered to be $E_s = 2E+08(kPa)$, Poisson's ratio $\upsilon = 0.3$ and density $\gamma_S = 78(kN/m^3)$. The liquid domain is modeled with three dimensional eight-node fluid element which is used to model contained fluids without any net flow rate. The utilized fluid element also includes special surface effects, which may be thought of as gravity springs used to hold the surface in place. The interaction between the tank and the liquid is accounted by properly coupling the nodes

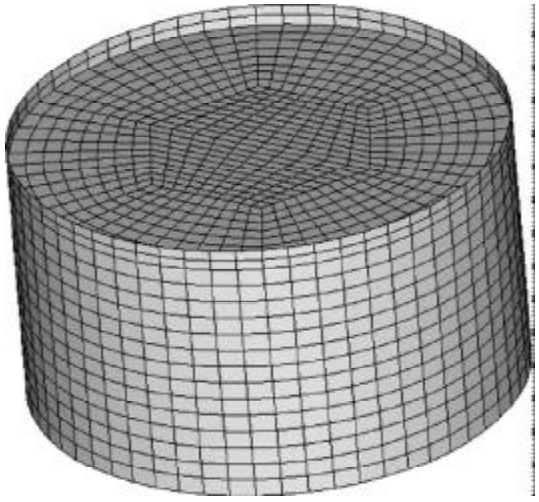

a) FEM mesh for bidirectional excitation.

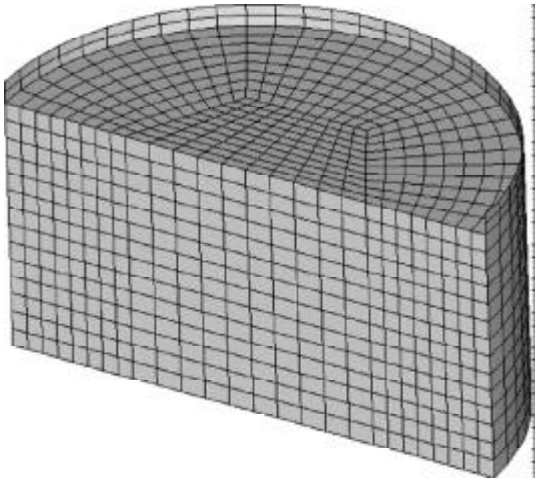

b) FEM mesh for unidirectional excitation.

Figure 2. Geometrical models for FEM analysis.

that lie in the common faces of these two domains. This means that the liquid can not be separated from the shell wall, but can move in the transverse directions and exerts only normal pressures to the tank wall. This assumption is also used in the formulation of the mechanical simplified model by Housner [17]. This approximation of linear behavior of the liquid simplifies the modeling of fluid-structure interaction.

4. Verification of the FEM Strategy

Prior to the use of the *FEM* for a parametric study on storage tanks, the accuracy of the introduced modeling strategy is investigated in this section. For this purpose, the results of free surface displacement obtained from the numerical model, is compared with experimental results reported by Chalhoub [28]. The test structure used here is a cylindrical steel tank, with a height of 60.96*cm* and a wall thickness of 1*mm* and a diameter of 121.92*cm*, similar to the experiment. The *El* Centro earthquake record scaled by peak acceleration 0.114*g* is considered as an input base excitation for the *FE* analysis.

The *FEM* results of free surface displacement are compared to free surface water elevation measured at a specific point of the shell wall for both the scaled tank and analytical solution given by Eq. (11). Corresponding results are illustrated in Figure (3). The first three modes (I = 1, 2, 3) are used to calculate the free surface theoretical solution. As Figure (3) shows, there is a good agreement between *FEM* results, the analytical solution and the experimental measurements. A maximum difference of 17% is calculated between *FEM* results and the measured peak free surface height. These levels of discrepancy are unavoidable because of the measurements difficulties and the assumptions made in the *FEM*.

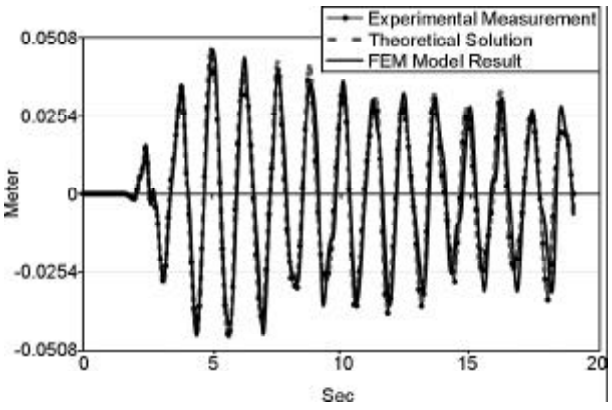

Figure 3. Comparing between FEM model results of sloshing wave height, experimental measurements and analytical solution (meter).

5. Parametric Studies Using FEM

As mentioned before, one of the main objectives of this article is to study the effects of the two components of earthquakes which are simultaneously exerted on storage tanks. For this purpose, five tanks with various aspect ratios are utilized. Dimensions and other geometrical characteristics of these tanks are listed in Table (1). Four earthquake base excitations are also utilized as input excitation of the system in which the peak ground accelerations have been considered between 2.62 to 8.3m/s^2. The earthquake specifications used for the time history analysis have been tabulated in Table (2). Acceleration response histories for the X-component of earthquakes have been plotted in Figure (4). As mentioned before, this study aims to understand the differences between the results of *FEM* analysis and the simplified model and investigate the effect of multi-directional excitation. Therefore, in this work the relative value of sloshing wave height is more important than the absolute value of sloshing wave height. Hence, both low and high predominate frequency earthquake are selected as an input excitation. Among these seismic records, the *CHI* earthquake with predominant period at about 1.14*S* has a long period motion.

The soil-structure interactions is not considered in this study. In order to evaluate the effects of various components of earthquake accelerations on *MSWH*, both unidirectional horizontal accelerations

Table 1. Geometry dimensions of the tanks (meter).

	H/R	Radius of Tanks	Liquid Height	Lower Shell Thickness	Upper Shell Thickness
Tank 1	0.3	54.5	15.85	0.03	0.01
Tank 2	0.5	40	20	0.02	0.01
Tank 3	1	37	37.4	0.033	0.015
Tank 4	2	7.5	15	0.01	0.006
Tank 5	2.6	2.5	6.5	0.006	0.006

Table 2. Specifications of considered earthquakes.

Earthquake	Year	PGA*(M/S^2) X-Dir	PGA*(M/S^2) Y-Dir	Predominant** Period (Sec) X-Dir
Kocaeli	1999	2.62	3.42	0.9
Chi-Chi	1999	4.09	3.41	1.14
Tabas	1978	8.3	8.2	0.15
Northridge	1994	5.9	8.26	0.3

* Peak Ground Acceleration

** The predominant period is the period at which the maximum spectral acceleration occurs in an acceleration response spectrum calculated at 0.5% damping.

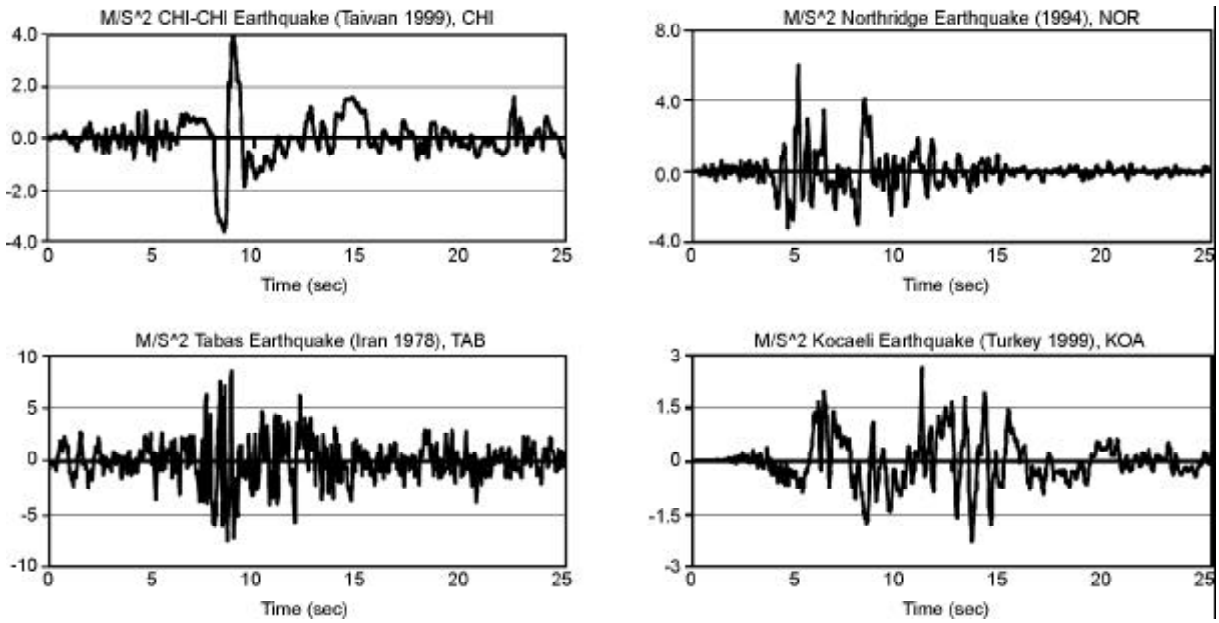

Figure 4. Ground acceleration time histories of considered earthquakes.

and bidirectional horizontal acceleration are separately exerted on the tank model. The results are explained in the following section.

5.1. Unidirectional and Bidirectional Excitation Results

Despite of unidirectional excitation, the free surface displacement response is no longer symmetric and the *MSWH* do not exactly occur at the same positions where *MSWH* of unidirectional excitation occurs, see Figures (5) and (6). The results of *FEM* for unidirectional excitation have been tabulated in Table (3) and are compared with the results of bidirectional excitation in Table (4).

Table (4) shows that the *MSWH* caused by two components of earthquake could be increased up to 65% respect to unidirectional excitation results. Therefore, the three-dimensional nature of the earthquake should be taken into account for the purpose of determining the *MSWH*.

5.2. Accuracy Assessment of Practical Formula for Unidirectional Excitation

Eq. (14) has been previously proposed for preliminary estimation of *SWH* and is used as a practical formula for design of cylindrical liquid storage tanks. The term $A_{con}(t)$ in Eq. (14) is generally evaluated using a specified earthquake response spectrum defined by codes. The spectral acceleration $A_{con}(\omega_\chi,\zeta)$ corresponds to the maximum acceleration arising in a lightly damped single-degree-of-freedom system of natural frequency ω_χ damping ratio ζ and subject to a unit peak ground acceleration.

The accuracy of Eq. (14) has been assessed by comparing its result with the results of *FE* analysis for unidirectional excitation (X-component), Table

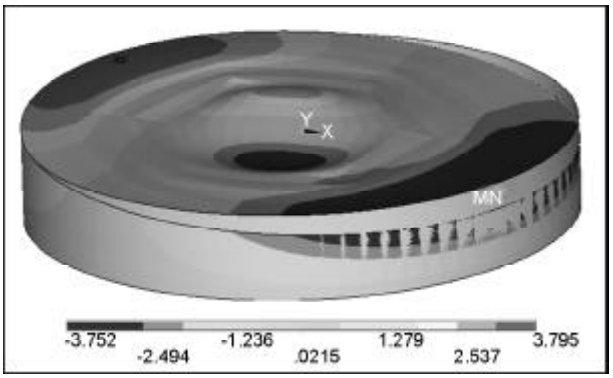

Figure 5. MSWH of Tank 1 subjected to two components of CHI earthquake.

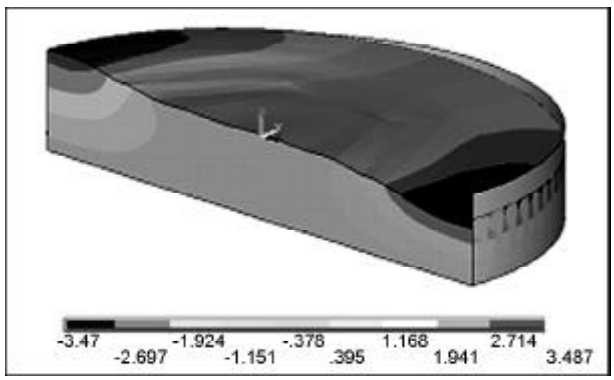

Figure 6. MSWH of Tank 1 subjected to one horizontal component of CHI earthquake.

Table 3. Comparison of MSWH obtained from unidirectional excitation FEM with results obtained of Eq. (14), Error= [(FEM-Eq14)/FEM] *100%.

		CHI		NOR		TAB		KOA	
		Middle	Side	Middle	Side	Middle	Side	Middle	Side
Tank 1	FEM Result	-	3.48	-	0.67	3.00	1.73	2.42	1.14
	Eq. (14)		3.59		0.16		1.26		0.64
	Error (%)		***-3.2***		***75.5***		***27.2***		***43.9***
Tank 2	FEM Result	-	7.10	-	0.73	2.90	2.50	2.18	1.28
	Eq. (14)		6.46		0.25		2.11		1.09
	Error (%)		***9.0***		***65.8***		***15.6***		***14.8***
Tank 3	FEM Result	-	8.56	-	0.91	3.35	3.02	2.40	1.6
	Eq. (14)		7.64		0.32		2.65		1.74
	Error (%)		***10.7***		***64.8***		***12.3***		***-8.7***
Tank 4	FEM Result	-	2.11	-	0.84	-	2.87	-	2.63
	Eq. (14)		1.56		0.64		3.18		2.58
	Error (%)		***26.1***		***23.8***		***-10.8***		***1.9***
Tank 5	FEM Result	-	2.06	-	1.36	-	1.23	-	0.96
	Eq. (14)		1.86		1.33		1.30		0.92
	Error (%)		***9.7***		***2.2***		***-5.7***		***4.2***

Table 4. Comparison of MSWH from unidirectional and bidirectional excitation Error Percentage = [(Bi-Uni)/Uni*100]%.

		CHI		NOR		TAB		KOA	
		Middle	Side	Middle	Side	Middle	Side	Middle	Side
Tank 1	Biaxial		3.79		1.02	3.07	1.75	2.55	1.18
	Uniaxial		3.48		0.67	3.00	1.73	2.42	1.14
	Error (%)		***8.9***		***52.2***	***2.3***	***1.2***	***5.4***	***3.5***
Tank 2	Biaxial		8.07		1.01	3.00	2.53	2.40	1.53
	Uniaxial		7.10		0.73	2.90	2.50	2.18	1.28
	Error (%)		***13.7***		***38.4***	***3.4***	***1.2***	***10.1***	***19.5***
Tank 3	Biaxial		9.91		1.38	3.40	3.07	2.52	2.24
	Uniaxial		8.56		0.91	3.35	3.02	2.40	1.60
	Error (%)		***15.8***		***51.6***	***1.5***	***1.7***	***5.0***	***40.0***
Tank 4	Biaxial		3.48		1.23		2.90		2.72
	Uniaxial		2.11		0.84		2.87		2.63
	Error (%)		***64.9***		***46.4***		***1.0***		***3.4***
Tank 5	Biaxial		2.98		2.19		1.42		1.00
	Uniaxial		2.06		1.36		1.23		0.96
	Error (%)		***44.7***		***61.0***		***15.4***		***4.2***

(3). According to this table, the prediction of Eq. (14) is less than *FEM* analysis for most of the tanks. The average errors percent for the tanks 1 to 5 are 37.4, 26.3, 24.5, 10.65 and 5.46 respectively. The accuracy of Eq. (14) is decreased by decreasing the period of first sloshing mode of the tanks, see Figure (7). This is due to the fact that Eq. (14) only considers first sloshing modes of the tanks. Therefore, the accuracy of this formula increases when the first sloshing period of tanks become closer to the predominant period of excitations.

It is noticeable that *MSWH* calculated by Eq. (14) is related to sloshing wave occurring at the tanks wall. However, the *MSWH* which obtained from *FEM* may takes place either in the middle of free surface, see Figure (8), or at the tank walls, see Figure (9). Because the *MSWH* in the middle of the tank may become important for flat roof tanks (with or without interior columns), the *MSWH* occurring in the middle of liquid free surface is also reported in mentioned tables.

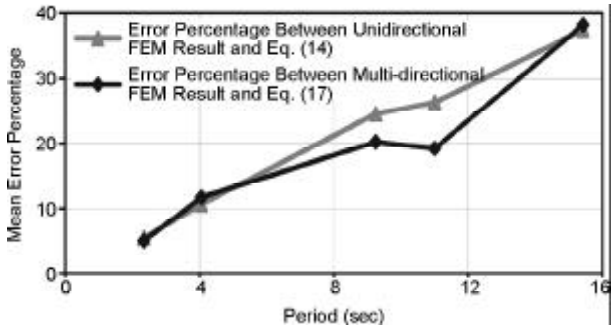

Figure 7. Mean Error of FEM results and theoretical solution, see Eq. (14), for MSWH.

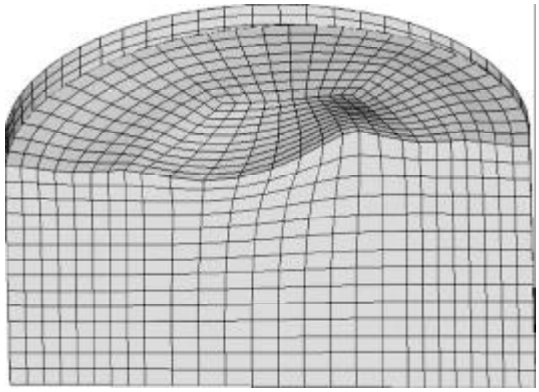

Figure 8. Tank 3 under KOA earthquake (MSWH occurs in the middle of tank).

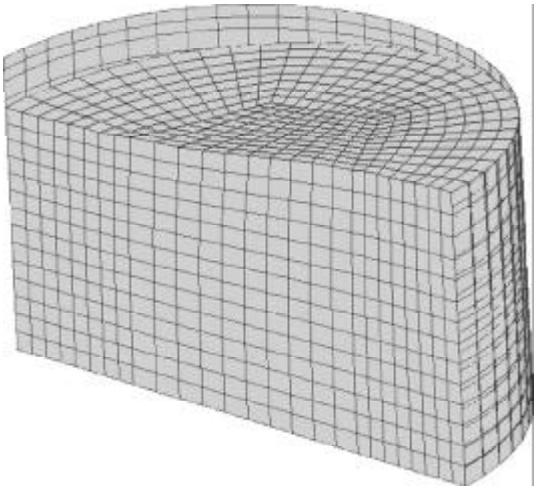

Figure 9. Tank 3 under CHI earthquake (MSWH occurs in the side wall of tank).

6. Assessment of Design Guideline Codes

In this section, the method of famous design codes and their relation to predict a *MSWH* is briefly discussed and their *MSWH* prediction values are compared with those obtained from *FEM* analyses of selected tanks.

In order to evaluate the accuracy of codes predictions, the spectral acceleration of the earthquakes should match the design spectrum of each code. But full matching of spectrums without substantially modifying the shape and energy content in the total frequency range of each ground motion is a very difficult issue and is not considered in this study. The justification is that the first-mode sloshing period in a large storage tank is very high and the associated damping of the sloshing motion is very small. These characteristics of liquid sloshing distinguish seismic response analyses of liquid storage tanks from response of typical elastic structures. Fundamental vibration period of typical structures are usually less than 2 seconds, and may present 5 to 10 percent of critical damping. Also, the strong-motion earthquake records have traditionally been made with the needs of building designers in mind, rather than with specific attention to the sloshing problem. Consequently, typical strong motion earthquake records may not accurately represent low frequency processes which can be of significance in exciting sloshing response. Therefore, a comparison between the results of design code prediction and *FEM* is just to evaluate the behavior of codes with respect to real earthquakes motion.

All design codes for calculating *MSWH* are developed based on convective mode base shear coefficient. Therefore, the evaluation of the *MSWH* requires a ground acceleration value corresponding to that particular mode of liquid deformation. The design guidelines considered in this study and their expressions to evaluate *MSWH* are tabulated in Table (5) and described as follows.

The design of tanks in the petroleum industry is referred to the standards published by *API* standard *API* 650 [29] titled Welded Steel Tanks for Oil Storage. Appendix *E* of this standard (*API*650) covers the seismic design provisions. The *ASCE*7 [30] procedure for tank design applies to general storage tanks while some special tanks are addressed to their appropriate codes. Tanks used for water storage are referred to the *AWWA*. The *ANSI/AWWA D*-100 [31] titled Welded Carbon Steel Tanks for Water Storage updated seismic design parameters. *AWWA* also is published standards for concrete reservoirs, *AWWA D*110 [32] and *AWWA D*115 [33] which is parallel to *ACI* 350.3 [34].

ASCE 7 and *API* 650 suggest the sloshing wave height as $A_c R_o L_{wc}$ and *D*-100 use $A_c R_o L_{wc}$, where L_{wc} is the response modification factor for the convective mode. *ACI* 350.3 and *D*-110 give the *MSWH* as $A_c R_o$, where A_c is the convective mode base shear coefficient and R_o is the radius of the tank. Additionally, Eurocode 8 suggests *MSWH* as $0.84\, A_c R_o$ [35]. The *D*-115 does not give any explicit expression for *MSWH* and refers that the *MSWH* is evaluated based on Housner method [18].

A comparison between the results of *MSWH* predicted by various codes and *FEM* for bidirectional excitation is tabulated in Table (6). Comparison of the values in this table shows that most of the mentioned design codes are not able to predict *MSWH* similar to the *FEM*. Therefore we should be

Table 5. Details of code expressions for evaluation of MSWH.

	Relation for MSWH	Convective Mode Base Shear Coefficient	Assumed Values for Parameters
ASCE7	$A_cR_oR_{wc}$	$Ac=\frac{1.5^{*}S_{D1}IT_L}{T_c^{\,2}}$ I is the importance factor; R is response modification factor; T_i is natural period of impulsive mode; T_c is natural period of convective mode; S_{DS} and S_{D1} are design spectra response coefficients; $Ts=S_{D1}/S_{DS}$; T_L is transition period for long-period range; and S_1 is the mapped maximum considering earthquake spectral response acceleration at a period of 1 s.	S_S=1.5,S_1=0.6,F_a=0.8,F_V =0.8, Site Class A, I=1.25, T_L=4s $S_{DS}=2/3F_aS_S$, $S_{D1}=2/3F_VS_1$
Eurocode 8	$0.84A_cR_o$	$Ac=g_1S_e,\ S_e=as\left(1+\frac{T}{T_B(2.5h-1)}\right)0\le T\le T_B,\ \ S_e=2.5ash\quad T_B\le T\le T_c$ $S_e=2.5ash\left(\frac{T_c}{T}\right)\ \ T_c\le T\le 3,\ S_e=7.5ash\left(\frac{T_c}{T^2}\right)\ \ T_c\le T\le 3\ and\ \ h=\left(\frac{7}{2+x}\right)^{0.5}$ a is peak ground acceleration factor; S is soil factor; ? is damping factor; *?* is viscous damping ratio; q is behavior factor; T is natural period; and T_B and T_c are periods at which constant-acceleration and constant-velocity range begin, respectively.	a =0.3, S=0.8, ? =1.2, T_B=0.15, T_C=0.6, q=2, subsoil class A
ACI350.3	A_cR_o	$Ac=\frac{1.875ZIS}{T_c^{\,2/3}}\quad for\ T_c\le 2.4.\quad A_c=\frac{6ZIS}{T_c^{\,2}}\quad T_c\succ 2.4$ Z is zone factor; S is soil factor; I is importance factor	Z=0.4, I=1.25, S=1,Soil type A
D110	A_cR_o	$A_c=\frac{4ZIS}{R_cT_c^{\,2}}$	Same as ACI350.3
D100	$1.4A_cR_oR_{wc}$	**Error! Objects cannot be created from editing field codes.**	Same as ASCE7
API650	$A_cR_oR_{wc}$	$Ac=\frac{1.5S_{D1}I}{T_cR_{wc}}\quad for\ T_c\le T_L\qquad \frac{1.5S_{D1}IT_L}{T_c^{\,2}R_{wc}}\quad T_c\succ T_L$	Same as ASCE7

Note: R_c, R_c, and R_w are response modification factors; S_{DS} and S_{D1} are design spectra response coefficients; $Ts=S_{D1}/S_{DS}$; T_c is natural period of convective mode; and T_L is transition period for long-period range.

Table 6. Comparison of sloshing wave height between various codes and FEM results (meter).

		Tank 1	Tank 2	Tank 3	Tank 4	Tank 5
Period of First Convective Mode (sec)		15.4	11	9.2	4.05	2.34
American Codes	ASCE7	0.545	0.792	1.036	1.095	0.640
	ACI350.3	0.687	0.992	1.300	1.370	1.328
	D110	0.460	0.661	0.867	0.913	0.913
	D100	0.545	0.792	1.036	1.095	0.640
	API650	0.545	0.792	1.036	1.095	0.640
Eurocode	CHI	0.43	0.62	0.82	0.85	0.67
	NOR	0.83	1.20	1.60	1.66	1.30
	TAB	1.17	1.69	2.25	2.34	1.83
	KOA	0.37	0.54	0.71	0.74	0.58
Finite Element Results	CHI	3.79	8.07	9.91	3.48	2.98
	NOR	1.02	1.01	1.38	1.23	2.19
	TAB	3.07	3	3.4	2.9	1.42
	KOA	2.55	2.4	2.52	2.72	1

careful to use code prediction while calculating *MSWH*. The convective forces may not be seriously affected by neglecting higher sloshing modes, while free surface displacements could be strongly affected by an excitation with substantial energy at higher-mode frequencies. However, the estimations of *ACI* 350.3 for *MSWH* are higher than those of other American codes.

In the *EC*8, *MSWH* is calculated as a function of the peak ground acceleration. Hence, a different *MSWH* value are predicted by this code for various earthquake types, while the prediction of other codes did not change for all input excitations. According to the *FEM* results, it seems that *MSWH* is affected by the nature of earthquake motion more than the effect of peak ground acceleration. Therefore, sloshing response is mainly affected by ground displacement rather than ground acceleration. In other words, the long-period strong motion could generate strong sloshing waves in large tanks. In this regard, imposing the peak ground acceleration factor for predicting *MSWH* is doubtful.

7. Extension of Practical Formulation for Bidirectional Excitation

The simplified Eq. (14) computes the *SWH* for each horizontal earthquake component along the *x* or *y* axis. Here it is assumed that the resultant *SWH* due to the two components of earthquake, could be calculated from superposition of each earthquake component effect as:

$$h_\theta(t) = h_x(t) + h_y(t) = \frac{0.84R}{g}\left(A_{c,x}(t)\cos\theta + A_{c,y}(t)\sin\theta\right) \quad (15)$$

Where $h_\theta(t)$ is the height of (*SWH*) on the tank wall in direction θ, R is the radius of the tank, $A_{c,x}(t)$ and $A_{c,y}(t)$ are directional acceleration of the convective part of liquid at time *t*. For tank 3 (as an example), the time history results of *SWH* obtained from Eq. (15) are compared with *FEM* results in Figure (10). As can be seen from this figure, superposition rule could be properly evaluated by the time history of free surface displacement.

Eq. (15) is suggested to calculate the time history values of free surface displacement in a particular point. However, from the design point of view, the maximum value of free surface displacement is required. Therefore, the absolute *MSWH* could be

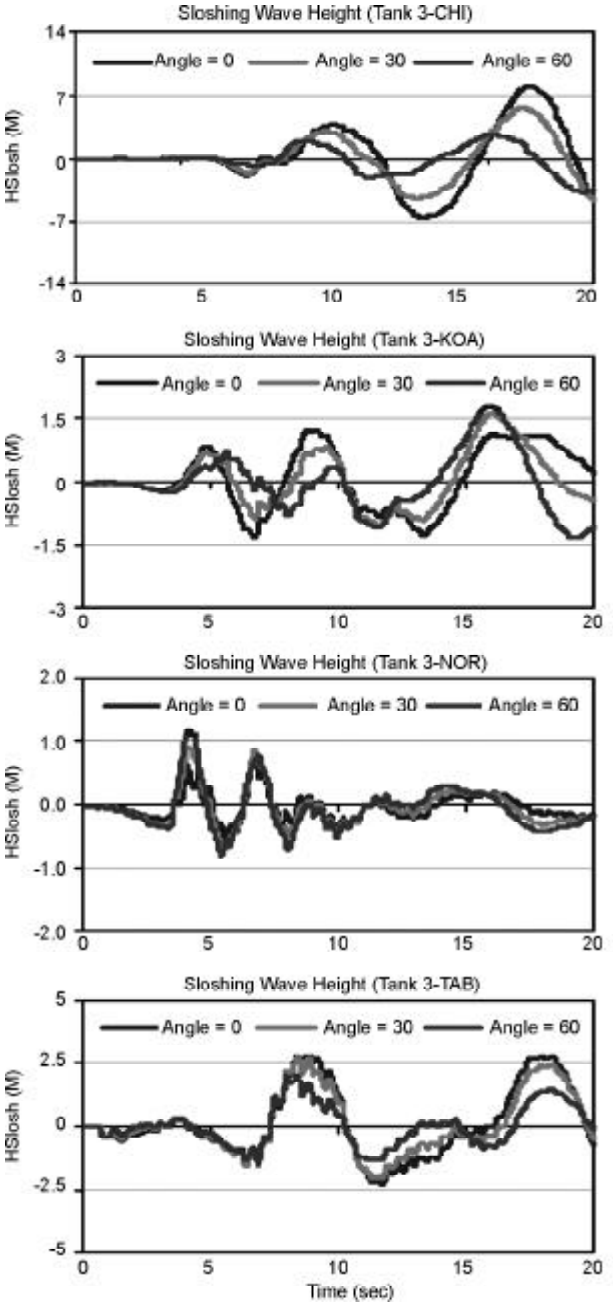

Figure 10a. Time history FEM result of SWH for different angle of tank 3.

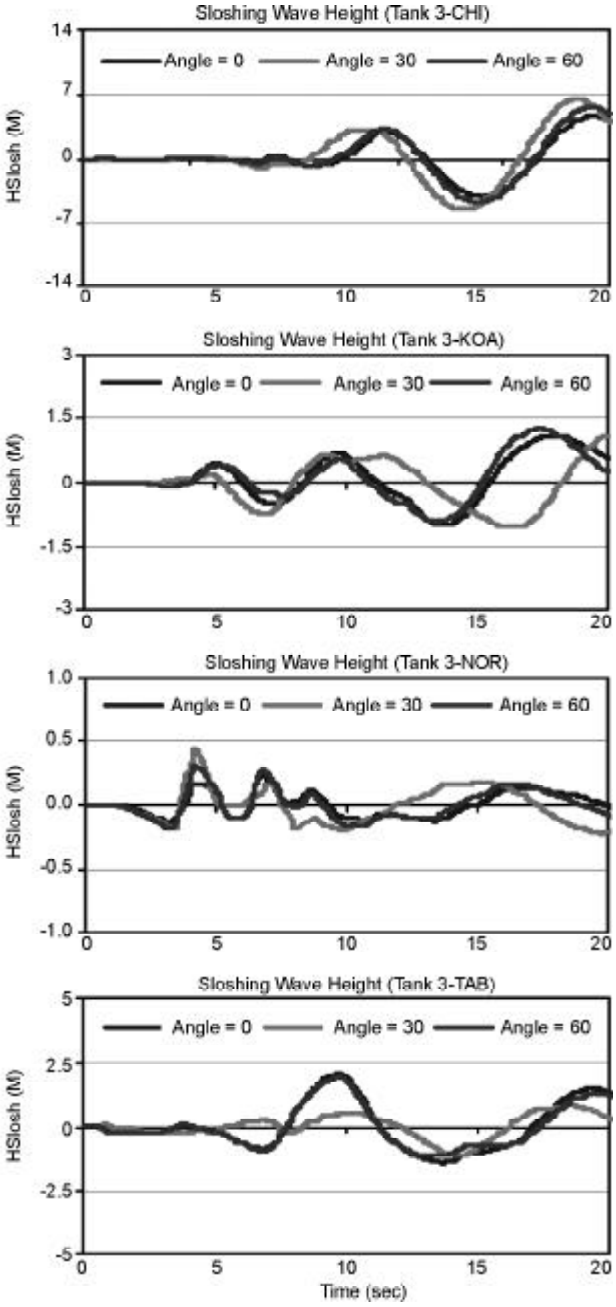

Figure 10b. Time history result of SWH obtained from Eq. (15) for different angle of tank 3.

extracted by derivation of Eq. (15) with respect to the direction angle α:

$$\frac{\partial h_\theta(t)}{\partial \theta} = \frac{0.84R}{g}\left(A_{c,x}(t).sin\alpha + A_{c,y}(t).cos\alpha\right)$$
$$\frac{\partial h_\theta(t)}{\partial \theta} = \frac{0.84R}{g} \Rightarrow tan\theta \frac{A_{c,y}(t)}{A_{c,x}(t)} \quad (16)$$

Substituting the above value into Eq. (15), the maximum sloshing wave height can be obtained as:

$$h_{max}(t) = \frac{0.84R}{g}\left(\frac{\left(A_{c,x}(t)\right)^2 + \left(A_{c,y}(t)\right)^2}{\sqrt{\left(A_{c,x}(t)\right)^2 + \left(A_{c,y}(t)\right)^2}}\right) \quad (17)$$

A comparison of time history results for *MSWH* at the side wall of tanks obtained from bidirectional *FEM* and Eq. (17) has been presented in Figures (11) to (13) as an example. It should be noted that the position of *MSWH* changes over time. The peak

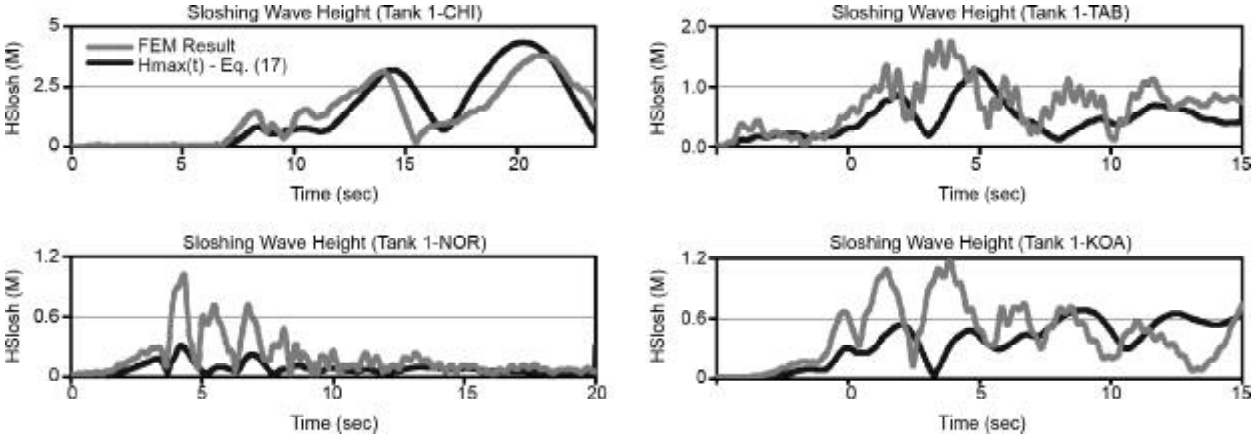

Figure 11. Time history results of MSWH under bidirectional earthquake motion (Tank 1).

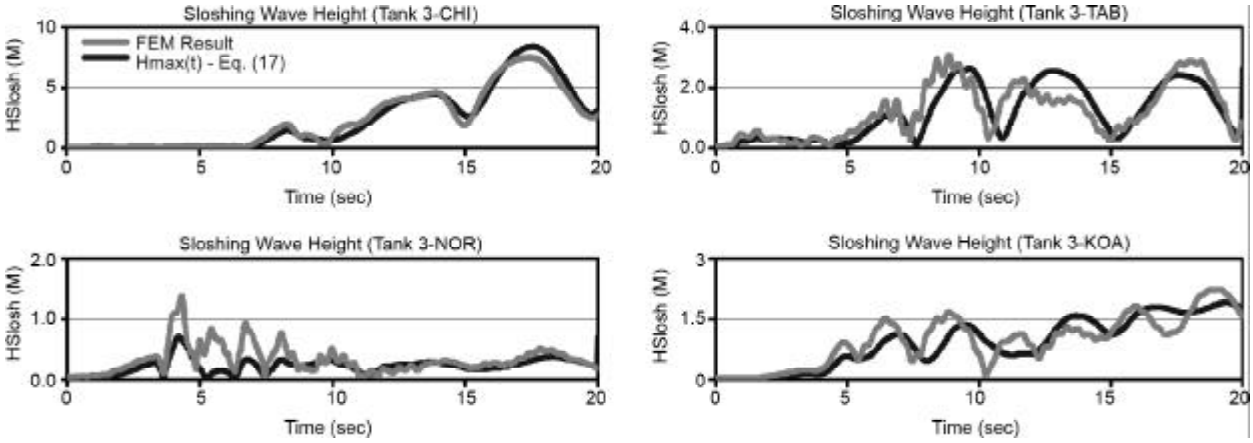

Figure 12. Time history results of MSWH under bidirectional earthquake motion (Tank 3).

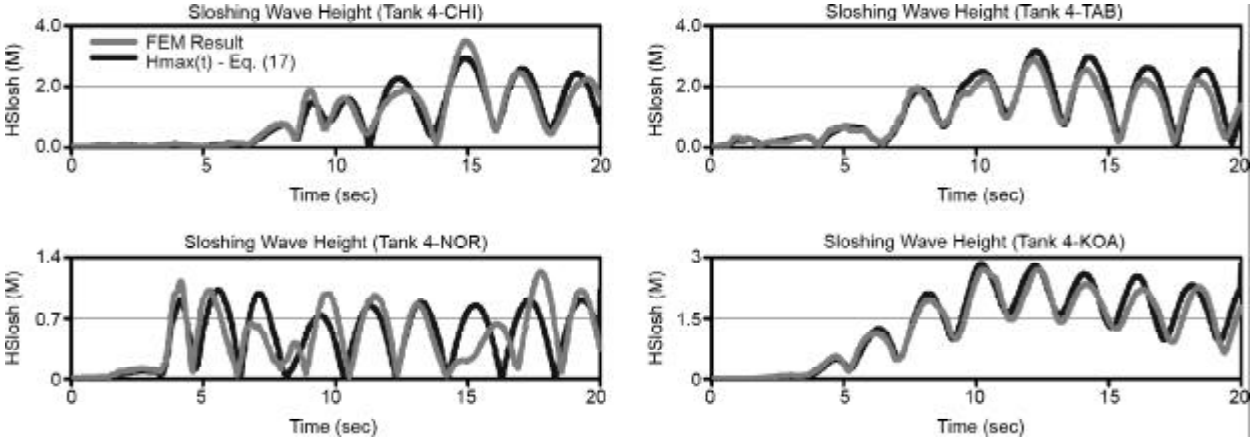

Figure 13. Time history results of MSWH under bidirectional earthquake motion (Tank 4).

values of *MSWH* for both *FEM* and Eq. (17) are also compared in Table (7). The mean absolute errors for tank 1 to 5 are 38.2, 19, 20, 12 and 5%, respectively. The relation between these errors and natural periods of first sloshing modes of the tanks is also illustrated in Figure (7). In this picture the similarity of the accuracy of unidirectional, see Eq. (14), bidirectional, see Eq. (17), and simplified formula with respect to *FEM* results could be observed. It should be noted that the error percentage between the results of sloshing wave height obtained from two dimensional *FEM* and simplified equation significantly depends on the dynamic characteristics of exerted excitation. This error could rise up to 55% for some base excitation, as reported by other researchers [36].

8. Summary and Conclusion

In this paper, *FEM* is used to investigate the effect of bidirectional excitation on *MSWH* of vertical, cylindrical tanks. First, the accuracy of the *FEM* strategy was validated. Then the five modeled tanks were considered for a parametric study using four earthquake acceleration records. The accuracy of practical formula is assessed by comparison with unidirectional Excitation. The accuracy of provisions, suggested by famous design codes for evaluation of *MSWH*, was assessed by comparing their results with *FEM*. Finally the results of unidirectional and bidirectional excitation were compared and a simplified method was proposed based on superposition rules to evaluate the effect of bidirectional excitation.

The main conclusions of this study may be summarized as follow:

- The comparison with experimental measurements reveals that the use of the considered *FEM* provides enough accuracy for evaluating seismic behavior of free surface waves in tanks.
- *MSWH* obtained from *FEM* occurs in the side wall of slender tanks. In media or broad tanks, however, it may occur in the middle of the free surface.
- Eq. (17) which is obtained based on superposing rules, is suggested here for evaluating *MSWH* of cylindrical tanks under bidirectional excitation.
- Comparison of computed results of the *MSWH* obtained from *FEM* analysis using unidirectional and bidirectional earthquake accelerations showed that considering simultaneous effect of earthquake components may end up with 65% for *MSWH*. Therefore, the multi-dimensional nature of the earthquake motion should be taken into account.
- The accuracy of the simplified Eq. (14) for unidirectional excitation, and Eq. (17) for bidirectional excitation was linearly decreased by decreasing of the first sloshing modes period of the tanks. The average absolute error between the results of *FEM* and those obtained from these simplified equations, see Eqs. (14) and (17), were calculated as 20.8 and 19.4% respectively for the fixed modeled tanks and excitations in this study.
- The maximum free surface displacements obtained from bidirectional finite element analysis did not lie in the range of the code predictions.
- Long period ground motion was the main parameter which affects sloshing wave height. This may be due to the fact that *MSWH* was influenced by the nature of earthquake motion rather than the effects of other seismic characteristics such as, peak ground acceleration. Thus, based

Table 7. Comparison the MSWH results of FEM and Eq. (17) for bidirectional excitation Error Percentage = [(FEM-Eq17)/FEM*100]%.

		CHI		NOR		TAB		KOA	
		Middle	Side	Middle	Side	Middle	Side	Middle	Side
Tank 1	FEM Result		3.79		1.02	3.07	1.75	2.55	1.18
	Eq. (17)	-	4.33		0.30		1.28		0.68
	Error (%)		**-14.2**		**70.6**		**26.9**		**42.4**
Tank 2	FEM Result		8.07		1.01	3.00	2.53	2.40	1.53
	Eq. (17)	-	7.80		0.50		2.11		1.43
	Error (%)		**3.3**		**50.5**		**16.6**		**6.5**
Tank 3	FEM Result		9.91		1.38	3.40	3.07	2.52	2.24
	Eq. (17)	-	9.61		0.70		2.65		1.92
	Error (%)		**3.0**		**49.3**		**13.7**		**14.3**
Tank 4	FEM Result		3.48		1.23		2.90		2.72
	Eq. (17)	-	2.96		1.03		3.20		2.84
	Error (%)		**14.9**		**16.3**		**-10.3**		**-4.4**
Tank 5	FEM Result		2.98		2.19		1.42		1.00
	Eq. (17)	-	3.13		2.07		1.46		0.93
	Error (%)		**-5.0**		**5.5**		**-2.8**		**7.0**

on the results of this study, the method of *EC*8 code for imposing a peak ground acceleration factor to predict *MSWH* seems to be not necessary.

Acknowledgements

This work was carried out as a part of the contract awarded by the National Iranian Oil Company (*NIOC*). Their financial support is gratefully acknowledged.

References

1. Bridges, T.J. (1982). "A Numerical Simulation of Large Amplitude Sloshing", *Proceedings of the 3rd International Numerical Ship Hydrodynamics*, Paris, 269-281.

2. Faltinsen, O.M. (1978). "A Numerical Non-Linear Method of Sloshing in Tanks with Two-Dimensional Flow", *J. of Ship Research*, **18**(4), 224-241.

3. Mikelis, N.E. (1984). "Sloshing in Partially Filled Liquid Tanks and Its Effect on Ship Motions: Numerical Simulations and Experimental Verification", RINA Spring Meeting, London.

4. Arai, M., Cheng, L.Y., and Inouc, Y. (1994). "3-D Numerical Simulation of Impact Load Due to Liquid Cargo Sloshing", *J. of the Society of Naval Architects of Japan*, **171**, 177-84.

5. Wu, G.X., Ma, Q.W., and Eatock-Taylor, R. (1998). "Numerical Simulation of Sloshing Waves in a 3D Tank Based on a Finite Element Method", Appl. Ocean Res 20, 337-355.

6. Faltinsen, O.M. and Rognebakke, O.F. (2000). "Sloshing", *International Conference on Ship and Shipping Research*, NAV, Venice, Italy.

7. Kim, Y. (2001). "Numerical Simulation of Sloshing Flows with Impact Load", Appl. Ocean Res., **23**, 53-62.

8. Kim, Y., Shin, Y.S., and Lee, K.H. (2004). "Numerical Study on Slosh-Induced Impact Pressures on Three-Dimensional Prismatic Tanks", Appl. Ocean Res., **2**, 213-226.

9. Colagrossi, A. and Landrini, M. (2003). "Numerical Simulation of Interfacial Flows by Smoothed Particle Hydrodynamics", *J. Comp. Phys.*, **19**, 448-475.

10. Iglesias, A.S., Rojas, L.P., and Rodriguez, R.Z., (2004). "Simulation of Anti-Roll Tanks and Sloshing Type Problems with Smoothed Particle Hydrodynamics", Ocean Eng., **31**, 1169-1192.

11. Oger, G., Doring, M., Alessandrini, B., and Ferrant, P. (2006). "Two-Dimensional SPH Simulations of Wedge Water Entries", *J. Comp. Phys.*, **213**, 803-822.

12. Kashiyama, K., Tanaka, S., and Sakuraba, M. (2003). "PC Cluster Parallel Finite Element Analysis of Sloshing Problem by Earthquake Using Different Network Environments", Communications in Numerical Methods in Engineering, **18**(10), 681-690.

13. Cho, J.R. and Lee, H.W. (2004). "Non-Linear Finite Element Analysis of Large Amplitude Sloshing Flow in Two-Dimensional Tank", *International Journal for Numerical Methods in Engineering*, **61**(4), 514-531.

14. Martin, J. (2006). "Application of a Discontinuous Galerkin Finite Element Method to Liquid Sloshing", *Journal of Offshore Mechanics and Arctic Engineering*, **128**, 1-10.

15. Hatayama, K., Zama, S., Nishi, H., Yamada, M., Hirokawa, M., and Inoue, R. (2005). "The Damages of Oil Storage Tanks During the 2003 Tokachi-Oki Earthquake and the Long Period Ground Motions", *Proceedings of the JSCE-AIJ Joint Symposium on Huge Subduction Earthquakes-Wide Area Strong Ground Motion Prediction*, In Japanese, 7-18.

16. Housner, G.W. (1954). "Earthquake Pressures on Fluid Containers", Report No. 081-095 Eighth Technical Report under Office of Naval Research, Project Designation, California Institute of Technology, Pasadena, California.

17. Housner, G.W. (1957). "Dynamic Pressures on Accelerated Fluid Containers", Bulletin of the Seismological Society of America, **47**(1), 15-35.

18. Housner, G.W. (1963). "Dynamic Analysis of Fluids in Containers Subjected to Acceleration", Report No. TID 7024, Nuclear Reactors and

Earthquakes, U.S. Atomic Energy Commission, Washington D.C.

19. Wozniak, R.S. and Mitchell, W.W. (1978). "Basis of Seismic Design Provisions for Welded Steel Oil Storage Tanks", *American Petroleum Institute 43rd Midyear Meeting*, Session on Advances in Storage Tank Design, Toronto, Canada.

20. Veletsos, A.S. and Young, T. (1977). "Earthquake Response of Liquid Storage Tanks", *Proc. of 2nd Engineering Mechanics Specialty Conf. ASCE Raleigh*, 1-24.

21. Haroun, M.A. and Housner, G.W. (1981). "Seismic Design of Liquid Storage Tanks", *J. of Technical Councils ASCE*, **107**(TC1), 191-207.

22. Veletsos, A.S. (1984). "Seismic Response and Design of Liquid Storage Tanks", Guidelines for Seismic Design of Oil & Gas Pipelines System, *ASCE*, NY, 255-370.

23. Malhotra, P.K., Wenk, T., and Wieland, M. (2000). "Simple Procedure for Seismic Analysis of Liquid Storage Tanks", *Structural Engineering, IABSE*, **10**(3), 197-201.

24. Malhotra, P.K. (2005). "Sloshing Loads in Tanks with Insufficient Freeboard", *Earthquake Spectra*, **21**(4), 1185-1192.

25. Malhotra, P.K. (2006). "Earthquake Induced Sloshing in Tanks with Insufficient Freeboard", *International Journal of Structural Engineering*, **16**(3).

26. Lamb Sir, H. (1945). "*Hydrodynamics*", 6th Ed., Dover Publications, Inc., New York.

27. Wiegel, R.L. (1964). "*Oceanographical Engineering*", Prentice Hall, Inc.

28. Chalhoub, M.S. (1987). "Theoretical and Experimental Studies on Earthquake Isolation and Fluid Containers", Ph.D. Dissertation, University of California, Berkeley.

29. American Petroleum Institute (API) (1998). "Welded Storage Tanks for Oil Storage", API 650, American Petroleum Institute Standard, Washington D.C.

30. American Society of Civil Engineers (ASCE) (2005). "Minimum Design Loads for Buildings and Other Structures", ASCE 7, ASCE Standard, SEI/ASCE 7-02, Reston, VA.

31. American Water Works Association (AWWA) (2005). "Welded Steel Tanks for Water Storage", AWWA D-100, Denver, CO.

32. American Water Works Association (AWWA) (1995). "Wire- and Strand-Wound Circular, Prestressed Concrete Water Tanks", AWWA D-110, Denver, CO.

33. American Water Works Association (AWWA) (1995). "Circular Prestressed Concrete Water Tanks with Circumferential Tendons", AWWA D-115, Denver, CO.

34. ACI 350.3 (2001). "Seismic Design of Liquid Containing Concrete Structures", An American Concrete Institute Standard.

35. Eurocode 8 (1998). "Design Provisions for Earthquake Resistance of Structures, Part 1-General Rules and Part 4 - Silos, Tanks and Pipelines", European Committee for Standardization, Brussels.

36. Chen, W. and Haroun, M. (1996). "Large Amplitude Liquid Sloshing in Seismically Excited Tanks", *Earthquake Engineering and Structural Dynamics*, (25), 653-669.